Engineering 5 (2019) 1171–1178

Contents lists available at ScienceDirect

Engineering

journal homepage: www.elsevier.com/locate/eng

Research
Vehicle Engineering—Article

# Explicit–Implicit Co-Simulation Techniques for Dynamic Responses of a Passenger Car on Arbitrary Road Surfaces

Hongzhou Hu *, Zhihua Zhong

*State Key Laboratory of Advanced Design and Manufacturing for Vehicle Body, Hunan University, Changsha 410082, China*

ARTICLE INFO

*Article history:*
Received 18 March 2018
Revised 25 November 2018
Accepted 15 December 2018
Available online 19 September 2019

*Keywords:*
Durability study
Dynamic responses
Passenger car
Explicit–implicit co-simulation
Contact-impact
Friction
Substructures

ABSTRACT

To study the durability of a passenger car, this work investigates numerical simulation techniques. The investigations are based on an explicit–implicit approach in which substructure techniques are used to reduce the simulation time, allowing full vehicle dynamic analyses to be performed on a timescale that is difficult or impossible with the conventional finite element model (FEM). The model used here includes all necessary nonlinearities in order to maintain accuracy. All key components of the car structure are modeled with deformable materials. Tire–road interactions are modeled in the explicit package with contact-impact interfaces with arbitrary frictional and geometric properties. Key parameters of the responses of the car driven on six different kinds of test road surfaces are examined and compared with experimental values. It can be concluded that the explicit–implicit co-simulation techniques used here are efficient and accurate enough for engineering purposes. This paper also discusses the limitations of the proposed method and outlines possible improvements for future work.



## 1. Introduction

In the vehicle industry, durability tests are performed in test tracks to reveal design flaws before the end products are finalized. These tests are conducted in the late phase of product development. The engineering works required to address any design flaw may lead to expensive verifications and delay the time to market. Proper definitions of loads and load cases are therefore essential for the development of economical and robust products. Among typical car manufacturers, reference loads from previously developed cars are used in new generations. However, reference loads may not reflect the modifications in the new generations and may lead to a mismatch of load definitions. Measurements can be performed to determine the actual load levels, and loads can be determined by analyzing the data collected in vehicles. However, this is a time-consuming process that requires access to the actual vehicles. In Refs. [1,2], measured signals were used for the analyses of suspension arms. In Ref. [3], measured signals in the wheels were applied in the suspension analysis.

Testing in test rigs is an alternative method of verification. The collected signals at the wheel centers are used as the driving signals to simulate road conditions, as in Ref. [4]. The collected load signals are often edited to increase the intensity of loading, such that the test durations are accelerated. In Ref. [5], an investigation was performed on the measured signals to obtain a simplified and accelerated load spectrum for the body fatigue bench test. Like the testing in test tracks, testing in a test rig occurs during the late phase of product development, and requires a physical prototype to be ready.

Software simulations are another common way to predict load levels. Simulation models can be built in the earlier phase of engineering, allowing the optimization and evaluation of different designs. One of the most widely used simulations for load predictions is the multibody simulation, in which vehicle models are built and simulated in different load scenarios.

This article describes the full vehicle road simulation of a C-type passenger car with deformable material definitions, simulated on six different road surfaces that cover the common durability cycles in real test tracks. The simulation results are compared with the measured signals from the road tests. This work demonstrates the efficiency, accuracy, and flexibility of running full vehicle simulations using the finite element model (FEM), without the compromises that are typically assumed in multibody simulations.

* Corresponding author.
*E-mail address:* huhz@dexiangroup.com (H. Hu).

https://doi.org/10.1016/j.eng.2019.09.003

## 2. Basic assumptions in the modeling and simulation of the physical problem

To be able to predict the actual responses of a sophisticated car system on arbitrary road surfaces, it is very important to define the mathematical model of the car–road system correctly. Of course, such a mathematical model would be very complicated, as the car itself is usually a complex system and the car-to-road interaction adds further complexity. However, for engineering purposes, not every detail is needed in the model, so the modeling of the actual physical system can be significantly simplified. To be specific, only the key components of the system that affect the system's main responses of engineering interest need to be considered. Thus, the following assumptions are made in this study.

First of all, only key components that are designed to take loads are modeled explicitly; all other components are modeled implicitly—for example, by adding equivalent masses to the attached key components. Examples of "key components" include the body frame and the suspension system, while examples of "other components" include the interior decoration components and the seat covers. Furthermore, it is assumed that this study is mainly concerned with a durability study of the body frame and the suspension system. Thus, the reliability of the mounting of the body appendages, such as the back mirrors, is not included in this study. It is then reasonable to implicitly model the front and rear bumpers by attaching equivalent masses to the front and rear longitudinal beams to which the bumpers are mounted.

Second, the tire–road interactions are modeled by frictional contact-impact between the tires and road surfaces. The tires are modeled in sufficient detail to capture realistic deformation during the interaction with the road surfaces. The steel wheel frame and the reinforcing steel wire are also modeled. However, the interactions between the steel wire and the rubber material of the tire are only approximated by tied interfaces in order to simplify the modeling. On the other hand, the road surfaces can be as detailed as may be desired; for example, it is possible to have an arbitrary geometry of the road surface with arbitrary frictional properties. Nevertheless, the road surface is assumed to be rigid, although it can be assumed to be elastic. Since the Young's modulus of the road surface is usually much larger than that of the tire, such an assumption will not introduce any significant error to the simulation. A simulation that considers deformation of road surfaces is more common in studies of all-terrain vehicles, such as in Ref. [6].

Third, it is assumed that no plastic deformation will occur during the simulation, although large deformation of the tires and suspension components is assumed. The spot-welding connections are modeled with tied interfaces of the relevant components, as are the bolted connections. It should be pointed out that the pin-ball joints and cylindrical joints must be modeled correctly in order for the responses of the car system to be predicted correctly. Another critical point is that the rubber buffering elements between the steel connections should also be modeled in detail in order to guarantee accurate results from the simulation.

Fourth, the behavior of all the materials of the components in the system is assumed to be within the elastic or viscous-elastic range. However, the model is not limited to elastic material behavior. In the case of overloading, regular elements can be applied in the studied regions with proper elastic-plastic material curves. The parameters of the material models are provided by the material suppliers, although the material behavior changes to some extent due to the forming process. All welding joints or other joints are assumed to be strong enough, such that no failure occurs during the simulation. Frictional conditions should be assumed in all joints involving relative movement, as well as between the tires and the road surface.

Finally, it is assumed that this study aims to explore the possibility of applying the simulation techniques to predict the dynamic responses of the car–road system. However, it is far beyond the capacity of a single article to address all the problems involved. Therefore, this study should be viewed as the most important basic step toward the final goal. Once it is shown that the responses can be predicted by the simulation techniques, further measures can be taken to use the model for durability analysis. For example, cyclic stress states may be estimated and the fatigue performance of the car system can be assessed using the simulation approach.

## 3. Common simulation techniques and their limitations

### 3.1. Common simulation techniques

Suspensions and vehicle bodies are exposed to a wide variety of loads, both from driveline and road–tire interactions. From a durability point of view, road profiles and road–tire interactions have a major impact in comparison with other loads (Fig. 1). Uncertainties and difficulties in determining proper load level or load cases usually lead to over-dimensioning, since conservative levels are often selected.

Multibody simulations are often performed under the assumption of rigid bodies. For parts that are stiff enough, and when the stiffness does not vary under the loading, such an assumption is often sufficient, as shown in Refs. [7,8]. However, due to the complexity of vehicle designs and load characters, vehicle components may behave nonlinearly. It is therefore necessary to include flexibility as well as other nonlinearities in the simulation models. The assumption of a rigid body is limited in applications where the flexibility of structures or other nonlinear effects are important. In some multibody programs, stiffness can be included by importing the neutral files generated by FEM software, as shown in Refs. [1–3,9,10]. However, this type of analysis is still limited to the linear response, and nonlinear effects are not included.

At the same time, FEM is widely used for structural analysis. FEM can handle both linear and nonlinear effects. This type of analysis can vary from linear static to nonlinear dynamic problems. Common sources of nonlinearity—such as material, geometry, and interactions—can be handled well in FEM. However, the simulation cost is sensitive to model size, especially when nonlinear effects are dominated. Therefore, FEM is mostly used for local component analysis.

Dynamic analyses can be performed with either an implicit or explicit solver. In an implicit dynamic analysis, equilibrium equations are solved in each increment; the cost related to each increment is high, and the model size has a major influence on the simulation time. However, the time increment can be large, since the implicit time integration is unconditionally stable. An explicit analysis is an iterative solver based on the central-difference

**Fig. 1.** A passenger car on a road test.

method. There is no need to solve the equilibrium equations, and the cost for each increment is low. However, the time increment in the explicit method is limited by the density and by the lowest element size in the model [11]. An explicit solver is suitable for solving a highly nonlinear problem, such as tire–road interactions. The most common application of an explicit analysis is in car crash simulations, where the time duration is on the order of milliseconds. For durability cycles, as the typical time duration is in seconds, control of a large amount of data is important.

A reasonable approach is to perform multibody simulations in FEM so that both the flexibility and nonlinear effects can be included. Several problems need to be overcome before successful simulations can be obtained: These include the control of the model size, the tire–road interaction, and an easy definition of flexible and rigid bodies.

### 3.2. Difficulties in full vehicle dynamic simulation

There are several difficulties in full vehicle road simulations, one of which is the modeling of the tires. All loads from the ground to the suspensions are transferred through the tires. In earlier days, tire modeling was based on empirical formulas, which have good accuracy as long as the tire–road interactions follow the same conditions as those the formulas were taken from. For arbitrary road conditions, it is more accurate to use FEM-based tire models. Tire modeling based on FEM can be found in Refs. [12,13], in which the tire responses under braking were studied. FEM-based tire modeling was used in the present work as well. The tire–road interaction is highly nonlinear and the explicit solver is more suitable than the implicit solver, which may have difficulty providing converged solutions.

Another difficulty in a full vehicle simulation is computation efficiency. While FEM offers the diversity to perform both linear and nonlinear analyses, the model size is usually big when parts are modeled in FEM, leading to a high simulation cost for dynamic analyses—especially for durability cycle simulations. Full vehicle simulations have been performed in the explicit code (LS-DYNA), as shown in Refs. [14,15]. It can be seen that the model details are relatively rough and the simulated timescale is short in these simulations. In order to perform successful full vehicle simulations in FEM, approaches are necessary that provide a balance between the accuracy and the computation time.

Implicit and explicit solvers can be combined to perform more advanced simulations (co-simulations), which are otherwise difficult to perform using any single package. A co-simulation can be run that combines different types of analysis, such as mechanical and fluid dynamics, mechanical and thermal analysis, and so forth. In Ref. [16], co-simulation was performed for mechanical and hydraulic systems on a full vehicle test rig to simulate durability cycles. In Refs. [17,18], implicit and explicit co-simulations were performed, albeit with many common assumptions such as rigid bodies and linear responses.

## 4. An explicit–implicit co-simulation approach based on substructure techniques

This article describes dynamic simulations of a C-type passenger car on arbitrary road surfaces. Full flexible parts were defined in the model, connected through various connector elements. The tire–road interactions were simulated in the explicit package and all other parts were simulated in the implicit package. Both analyses ran independently with different time increments, and data exchanges were performed internally at wheel centers at specified time points. Prior to the dynamic co-simulations, static analyses were performed in both packages, and the results were defined as the initial conditions of the dynamic analyses.

In the implicit part, the suspension components and car body were described as substructures. Compared with the original FEMs, the substructures have only degrees of freedom (DOFs) at the user-defined locations, leading to a substantial reduction of the model size.

Substructure is one part of the FEM. The DOFs in a substructure are divided into either internal DOFs ($u^{\mathrm{E}}$) or retained DOFs ($u^{\mathrm{R}}$), as shown in Fig. 2. The basic idea of the substructure technique is to describe the response of the original structure through the retained DOFs, as shown in Eq. (1).

$$[M]^{\mathrm{R}}\{\ddot{u}^{\mathrm{R}}\}+[C]^{\mathrm{R}}\{\dot{u}^{\mathrm{R}}\}+[K]^{\mathrm{R}}\{\Delta u^{\mathrm{R}}\}=\left\{\boldsymbol{F}^{\mathrm{R}}\right\} \tag{1}$$

where $[M]^{\mathrm{R}}$, $[C]^{\mathrm{R}}$, and $[K]^{\mathrm{R}}$ are the mass, damping, and stiffness matrixes, respectively, related to the retained DOFs, and $\left\{\boldsymbol{F}^{\mathrm{R}}\right\}$is the internal force vector.

The virtual works ($\delta W$) expressed in terms of retained and internal DOFs in static and dynamic cases are determined according to Eqs. (2) and (3), respectively.

$$\delta W_{\mathrm{stat}}=\begin{bmatrix}\delta u^{\mathrm{R}} & \delta u^{\mathrm{E}}\end{bmatrix}\left(\begin{Bmatrix}\Delta P^{\mathrm{R}}\\ \Delta P^{\mathrm{E}}\end{Bmatrix}-\begin{bmatrix}K^{\mathrm{RR}} & K^{\mathrm{RE}}\\ K^{\mathrm{ER}} & K^{\mathrm{EE}}\end{bmatrix}\begin{Bmatrix}\Delta u^{\mathrm{R}}\\ \Delta u^{\mathrm{E}}\end{Bmatrix}\right) \tag{2}$$

$$\begin{aligned}\delta W_{\mathrm{dyn}}=\begin{bmatrix}\delta u^{\mathrm{R}} & \delta u^{\mathrm{E}}\end{bmatrix}\Bigg(&\begin{Bmatrix}\Delta P^{\mathrm{R}}\\ \Delta P^{\mathrm{E}}\end{Bmatrix}-\begin{bmatrix}M^{\mathrm{RR}} & M^{\mathrm{RE}}\\ M^{\mathrm{ER}} & M^{\mathrm{EE}}\end{bmatrix}\begin{Bmatrix}\ddot{u}^{\mathrm{R}}\\ \ddot{u}^{\mathrm{E}}\end{Bmatrix}\\ &-\begin{bmatrix}C^{\mathrm{RR}} & C^{\mathrm{RE}}\\ C^{\mathrm{ER}} & C^{\mathrm{EE}}\end{bmatrix}\begin{Bmatrix}\dot{u}^{\mathrm{R}}\\ \dot{u}^{\mathrm{E}}\end{Bmatrix}-\begin{bmatrix}K^{\mathrm{RR}} & K^{\mathrm{RE}}\\ K^{\mathrm{ER}} & K^{\mathrm{EE}}\end{bmatrix}\begin{Bmatrix}\Delta u^{\mathrm{R}}\\ \Delta u^{\mathrm{E}}\end{Bmatrix}\Bigg)\end{aligned} \tag{3}$$

where $\Delta P^{\mathrm{R}}$ and $\Delta P^{\mathrm{E}}$ are nodal forces applied to retained and internal DOFs respectively.

By applying the principal of virtual work in the static case, the following relation is obtained:

$$\{\Delta u^{\mathrm{E}}\}=\left[K^{\mathrm{EE}}\right]^{-1}\left(\left\{\Delta P^{\mathrm{E}}\right\}-\left[K^{\mathrm{ER}}\right]\{\Delta u^{\mathrm{R}}\}\right) \tag{4}$$

However, the static modes may not be sufficient to define the dynamic response accurately. One technique to improve accuracy in the dynamic case is to augment the response within the substructure by including some generalized DOFs [19] together with the eigenmodes of the substructure, resulting in the following:

$$\{\Delta u^{\mathrm{E}}\}=\left[K^{\mathrm{EE}}\right]^{-1}\left(\left\{\Delta P^{\mathrm{E}}\right\}-\left[K^{\mathrm{ER}}\right]\{\Delta u^{\mathrm{R}}\}\right)+\{\phi^{\mathrm{E}}\}^{\alpha}q^{\alpha} \tag{5}$$

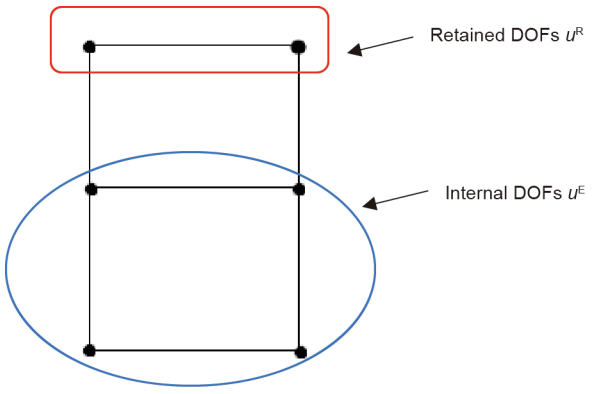


**Fig. 2.** A schematic representation of a substructure.

where $\{\phi^{E}\}^{\alpha}$ are the eigenmodes of the substructure, obtained with all retained DOFs constrained, and $q^{\alpha}$ are the generalized displacements.

Based on Eq. (5), the variation of the internal DOF and associated time derivatives is as follows:

$$\{\delta u^{E}\} = -\left[K^{EE}\right]^{-1}\left[K^{ER}\right]\{\delta u^{R}\} + \{\phi^{E}\}^{\alpha}\delta q^{\alpha}$$

$$\{\dot{u}^{E}\} = -\left[K^{EE}\right]^{-1}\left[K^{ER}\right]\{\dot{u}^{R}\} + \{\phi^{E}\}^{\alpha}\dot{q}^{\alpha}$$

$$\{\ddot{u}^{E}\} = -\left[K^{EE}\right]^{-1}\left[K^{ER}\right]\{\ddot{u}^{R}\} + \{\phi^{E}\}^{\alpha}\ddot{q}^{\alpha}$$

The internal DOFs and their time derivatives in Eq. (3) can therefore be replaced by the retained DOFs and the generalized displacements, reducing the system to the following:

$$W = \begin{bmatrix}\delta u^{R} & \delta q\end{bmatrix}\left([T]^{T}\{P\} - [T]^{T}[M][T]\begin{Bmatrix}\ddot{u}^{R}\\ \ddot{q}\end{Bmatrix} - [T]^{T}[C][T]\begin{Bmatrix}\dot{u}^{R}\\ \dot{q}\end{Bmatrix} - [T]^{T}[K][T]\begin{Bmatrix}\Delta u^{R}\\ \Delta q\end{Bmatrix}\right) \quad (6)$$

where $W$ is the virtual work,

$$[T] = \begin{bmatrix}[I] & [0]\\ -\left[K^{EE}\right]^{-1}\left[K^{ER}\right] & [\phi^{E}]\end{bmatrix},\ [M] = \begin{bmatrix}M^{EE} & M^{ER}\\ M^{RE} & M^{RR}\end{bmatrix},$$

$$[C] = \begin{bmatrix}C^{EE} & C^{ER}\\ C^{RE} & C^{RR}\end{bmatrix},\ \text{and}\ [K] = \begin{bmatrix}K^{EE} & K^{ER}\\ K^{RE} & K^{RR}\end{bmatrix}$$

and where $[I]$ is a unit matrix and $[0]$ is a null matrix.

There are many advantages to substructure techniques with regard to modeling and simulation time. In full vehicle simulation, the model size is usually large, leading to high simulation costs—especially in implicit dynamic analysis. At the same time, many parts may behave linearly in dynamic analyses. By identifying components that are suitable for substructure modeling, the simulation time can be significantly reduced, while the accuracy is maintained.

It is only necessary to generate the substructure once; thereafter, it can be used repeatedly. The same substructure can be shared by different simulation models, providing an economical way to model-share. For large models that are beyond the computational capability of the user's system, substructures can be used to build global models to keep the simulation cost low, while the outputs (stress/strain, etc.) of substructures can be recovered to study the local models in detail. However, the recovering process is a linear process. For nonlinear analysis, substructures can be combined with regular elements to ensure the accuracy of the analysis.

## 5. Modeling of a complete car–road system

Fig. 3(a) shows the complete vehicle model, and Fig. 3(b) shows the division of the co-simulation model into the explicit and implicit parts. Since the data exchanges between the parts occur at the wheel centers, it is important to ensure that the locations of the wheel centers are the same in the two packages at the start of the co-simulations. This can be achieved by, for example, using the same coordinates for the wheel centers in both packages and fixing the wheel centers in the static analyses (gravity load, inflation of tires, etc.).

### 5.1. Explicit part of the co-simulation

Fig. S1 in Appendix A shows the three-dimensional (3D) tire model, which was generated by revolving the two-dimensional (2D) cross-section of the tire. The cross-section includes the actual tire structure, such as rubber and steel reinforcements, as described in Ref. [18]. Fig. S2 shows the models of six road surfaces that correspond to the most common durability road types. General contacts were defined between the tires and the rigid road surfaces, with penalty formulation in the normal contact directions. A proper penalty factor of 0.1 was selected so that stabilized simulations were obtained.

### 5.2. Implicit part of the co-simulation

The implicit part of the co-simulation consisted of the front and rear suspensions—including the anti-rotation bars, shock dampers, and disk brakes—together with the sub-frames and the car body. All parts were connected through connector elements. The sub-frames, suspension components, and car body were described as substructures, with retained DOFs at their connection points. Fig. S3 shows the model of the rear sub-frame. The original model had over $1 \times 10^{5}$ DOFs; the number of DOFs in the corresponding substructure was $14 \times 6$.

Regular elements were assigned to the parts that may experience nonlinear deformations, such as the anti-rotation bars. In case other nonlinear effects were present, such as contact definitions during a braking load, the brake disks and pads were modeled with brick elements, as shown in Fig. S4. For parts that may experience overloading and plastic deformations, regular elements were also defined, together with nonlinear material

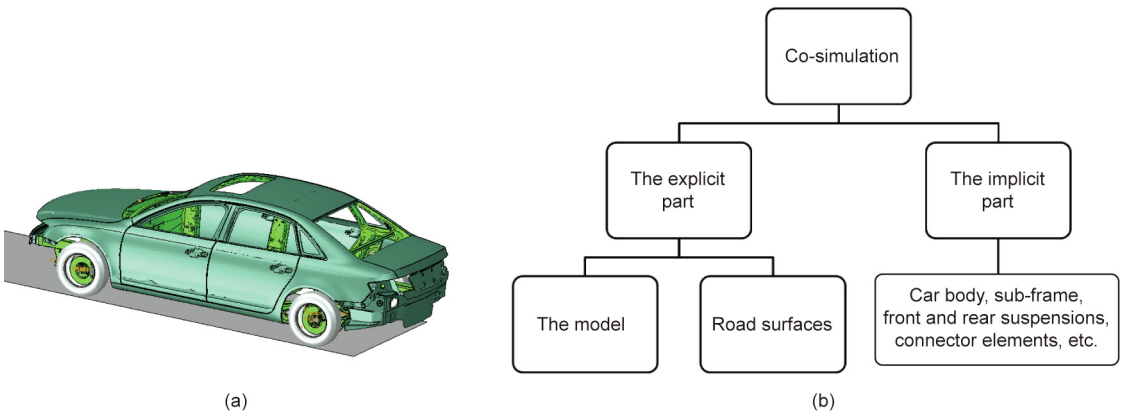


**Fig. 3.** Explicit and implicit co-simulation. (a) The complete model; (b) division of the co-simulation.

definitions. A combination of regular elements and substructures enables accurate and economical modeling.

There are a number of connections such as ball joints and bushings in the suspensions. The bushings have specified properties that are often nonlinear. Instead of modeling these bushings in detail, an economical and efficient way to define the connections is through the connector elements. Different properties—such as stiffness (Fig. S5), damping, friction, plastic deformation, failure criteria, and so forth—can be applied to the connector elements.

A small amount of Rayleigh damping was applied to damp both the low and high frequency. The energy level related to the damping energy is very small and does not affect the results. Hilber–Hughes–Taylor integration was used in the implicit dynamic simulation [20]. The algorithm itself introduces a small degree of numerical damping, which is suitable for contact simulations.

Table 1 provides a summary of the components in the complete co-simulation model. The total number of DOFs in the original model was over $2 \times 10^6$, of which the major portion was converted into substructures. After the conversion, the total number of DOFs in the implicit part of the co-simulation model was less than $2 \times 10^4$, with around $6 \times 10^4$ in the explicit part. Through a combination of substructures and regular elements in the co-simulation model, nonlinear dynamic analyses could be performed with reasonable simulation costs.

## 6. Simulation results with theoretical and experimental verification

At the beginning of the co-simulations, static analyses under the gravity loads were verified so that the static load distribution was correct. The results were used as the initial conditions of the dynamic analyses.

Fig. S6 shows the vertical accelerations of the shock-absorbing bar at the front suspension in three load cases. The peak levels are related to the time points when the tires were in contact with the obstacles of the road surface. Fig. S7 shows the force variations of the steering rod in different load cases.

The energy balance in the braking load case is shown in Fig. S8; it can be seen that the kinematic energy is decreasing and the friction dissipation energy is increasing, as expected. The stress/strain time history of the suspension components that were defined as substructures were recovered; two examples of the recovered stress plots are shown in Fig. S9.

As a verification, displacements of the wheel centers from the implicit and explicit packages were compared. Fig. 4 shows a comparison of the displacements in one of the wheel centers. It can be seen that the displacements from the two packages match well. However, there could be some mismatches ($\Delta^t$) in the rotational DOFs, as shown in Fig. 5(a), especially in the presence of highly nonlinear tire–road interactions (Fig. 5(b)). In that case, a small time increment was maintained to catch the nonlinearity at this moment.

**Table 1**
A list of components and their sizes in the FEM.

| Component | Original model DOFs | Corresponding substructure DOFs | Simulation package |
|---|---|---|---|
| Sub-frame (front) | $1.6 \times 10^5$ | $12 \times 6$ | Implicit |
| Sub-frame (rear) | $7 \times 10^4$ | $14 \times 6$ | Implicit |
| Car body | $5 \times 10^5$ | $23 \times 6$ | Implicit |
| Suspension parts | $4 \times 10^4$ each (average) | $4 \times 6$ each (average) | Implicit |
| Anti-rotation bars | 500 | — | Implicit |
| Brakes | $6 \times 10^3$ | — | Implicit |
| Tires | $6 \times 10^4$ | — | Explicit |
| Road surfaces | Rigid | — | Explicit |
| Bushings and other couplings | 1–6 each | — | Implicit |

## 7. Simulation result and experiment road testing

This section is divided into two subsections. The first subsection addresses the static verification of the tire and suspension stiffness, as these properties directly affect the accuracy of the simulation result. The second subsection is a comparison of the results of the dynamic road simulations and the testing.

### 7.1. Static verification: Tire and suspension

Kinematics is the study of motion due to geometry, and compliance is the deflection resulting from the application of a force. In kinematic and compliance (K&C) tests, important parameters of the suspension design are measured and validated. Fig. 6 shows the prototype car in the K&C test in which the tire and suspension stiffness are measured. In order to study the deformation characteristics of the front suspension, an FEM was built according to Fig. S10 and was analyzed entirely in the implicit package. The tire and suspension stiffness were measured and compared with the simulated results. Figs. S11 and S12 show a comparison of the tire and suspension stiffness, respectively, in the vertical direction. The simulated tire and suspension stiffness agree well with the corresponding measurements.

Strain gauges were placed on the front and rear suspension arms to monitor their strain levels. Fig. S13(a) shows one of the strain gauges, which was placed on the lower front suspension arm. The measured minimum principal strain level was −418 microstrain ($-4.18 \times 10^{-4}$) at the design suspension weight (1200 kg). Fig. S13(b) shows the stress plot at the same load level; the simulated minimum principal strain was −425 microstrain ($-4.25 \times 10^{-4}$). The static verification shows that the FEM has

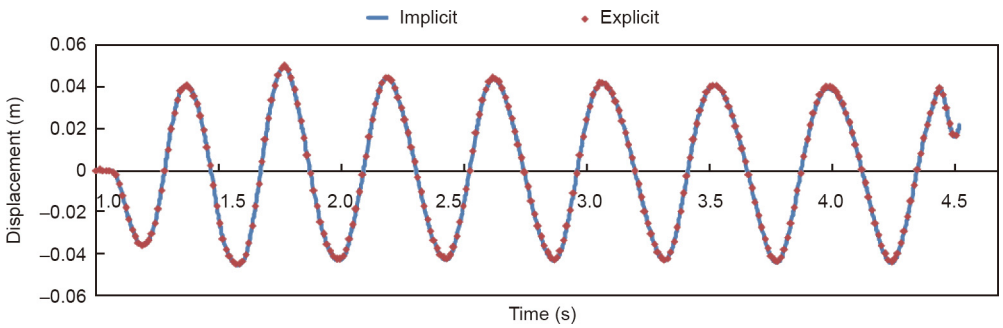


**Fig. 4.** A comparison of vertical displacements at one wheel center (torsional road).

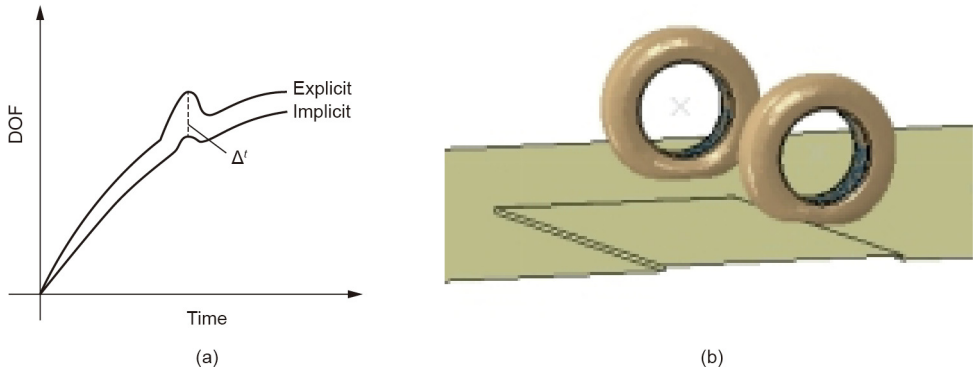


**Fig. 5.** Tire and road surface interaction. (a) DOF in wheel center; (b) tire–road interaction.

**Fig. 6.** The prototype car during the K&C test.

sufficient accuracy and that it provides a good basis for dynamic road simulations.

### 7.2. Dynamic road test and verification

The prototype car was equipped with an inertia sensor (RT2500) to record the velocities, accelerations, distances, and so forth in the durability testing. The device was placed between the two front seats, as shown in Fig. 7.

Fig. S14 shows an overview of the test field [21], which consists of five test loops, numbered F1 to F5. The F1 loop is the outer and longest loop. Fig. S15 shows two examples of road types in the durability test. Three road types (the vibration road, the washboard road, and the torsional road) in F1 were selected for a comparison of simulated and measured signals. These road types were selected because relatively good estimations could be obtained. Both the acceleration and the strain levels were analyzed, measured, and compared in the dynamic verification. Fig. 8 shows the forward vehicle velocity in the whole F1 loop, with the actual velocities on the three main road types marked. The average vehicle speed was around 10 $m \cdot s^{-1}$, except for the velocity on the torsional road. The measured and simulated vertical accelerations in the wheel center are shown in Fig. 9 and Fig. 10, respectively. The level crossings of the signals are shown in Fig. S16. It can be seen that the agreement is relatively good with regard to the maximum range.

The time histories of the maximum and minimum principal strains in the lower suspension arm on the torsional road were measured and compared with the simulated data (Figs. S17 and S18, respectively). It can be seen that the average strain levels of the measured and simulated strains are close, although the simulated strain ranges are higher than the measured levels. Upon close examination later, it was found that the damping coefficient in the shock observer model was higher than the actual level, which resulted in more rigid suspension stiffness in the dynamic scenario. This can partially explain the higher strain ranges in the simulation.

Although efforts were made to simulate the test cycles to be as close to reality as possible, many factors remained that could affect the results, such as mismatches in mass distribution, differences in vehicle speed, and geometrical differences of the road surfaces and tire properties. However, in general, it can be concluded that both the main features and the typical levels of the measured and simulated signals matched (or were close). Furthermore, it was found that there are significant advantages when performing full vehicle simulations with flexible parts and when including necessary nonlinear effects in an efficient manner.

**Fig. 7.** The prototype car equipped with an inertia sensor.

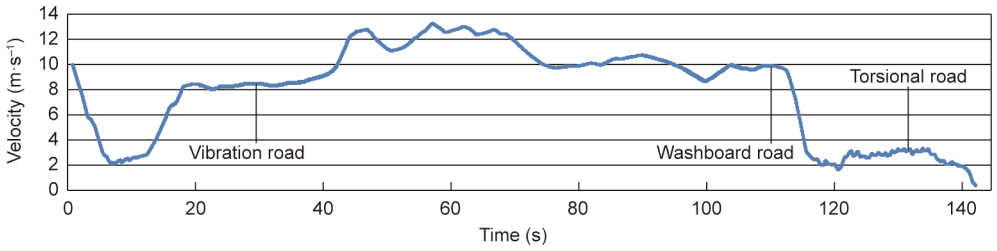


**Fig. 8.** Forward vehicle velocity (F1 test loop).

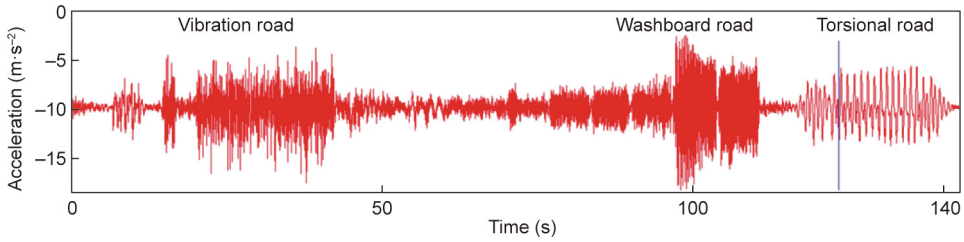


**Fig. 9.** Measured vertical acceleration in the vehicle center (F1 test loop).

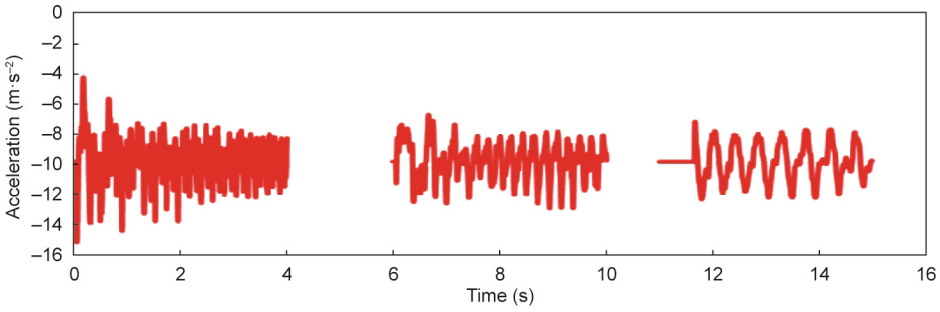


**Fig. 10.** Simulated vertical acceleration in the vehicle center (F1 test loop).

## 8. Concluding remarks

In conclusion, FEM is a standard analysis tool for linear and nonlinear analyses, and is a good candidate for multibody simulation, such as full vehicle durability simulation. However, there are limitations on the simulation efficiency. This article describes the techniques used for full vehicle simulation on arbitrary road surfaces, and demonstrates the efficiency of vehicle simulation without the common assumption of a rigid body and linear analysis.

Under linear conditions, the substructure technique can be used to replace the standard FEM with user-defined nodes. The model size can be significantly reduced, which permits much faster simulation. In a full vehicle simulation, by identifying parts that are suitable for substructure techniques, the overall simulation cost can be kept low, while a detailed analysis can be provided in the areas of interest.

Based on the features of the implicit and explicit analyses, co-simulations were run between the two analysis packages. The explicit solver was used to handle the complicated tire–road interactions, and the implicit solver was used to handle the large model (through substructures, etc.), while its efficiency was used to handle moderate nonlinearity in the dynamic analyses.

By combining multiple simulation techniques and strategically dividing the simulation model, a full vehicle model was built and simulated on arbitrary road surfaces, with acceptable results in terms of both efficiency and accuracy. This result indicates the possibility of using simulated loads in fatigue designs or/and strength checks, which will permit verification to be performed during an early phase of product development.

To obtain sufficient accuracy in dynamic simulations, it is recommended to perform static verification first. As shown in Section 7.1, the static verification showed good agreement, with a difference between the simulated and measured data of less than 5%. The dynamic study presented a greater difference as it was more complicated, but the result was still manageable, and potential improvements were identified. An average error below 10% should be possible to achieve in dynamic verification with carefully prepared inputs, systematic modeling, and simulations.

## Acknowledgements

This work is supported by Key Technology Research and Industrialization of the C-type passenger Car, Major Science and Technology Project of Chongqing Municipality, Mar 2012–Dec 2016.

## Compliance with ethics guidelines

Hongzhou Hu and Zhihua Zhong declare that they have no conflict of interest or financial conflicts to disclose.

## Appendix A. Supplementary data

Supplementary data to this article can be found online at https://doi.org/10.1016/j.eng.2019.09.003.

## References


[1] Qian L, Wu D, Yang N. Multiaxial fatigue analysis of vehicle lower control arm based on simulated road excitation. Automot Eng 2012;34(3):249–54. Chinese.
[2] Shi J, Guan X. Fatigue life analysis of lower suspension arm. Automot Eng 2013;35(3):256–60. Chinese.
[3] Feng J, Liu L, Zheng S. Load simulation analysis on a car suspension system. Automot Eng 2012;34(10):913–7. Chinese.
[4] Ren G, Tao Q, Yu W. Research on vehicle fatigue simulation and experimental study based on road load spectra. Chinese J Automot Eng 2013;3(4):300–4. Chinese.
[5] Gao Y, Xu C, Fang J. Study on the programmed load spectrum of the body fatigue bench test. J Mech Eng 2014;50(4):92–8. Chinese.
[6] Zhang X, Sun B, Xu Z, Chen N, Sun Q. Modeling and simulation of vehicle terrain coupling system considering terrain deformable characteristic. J Mech Eng 2009;45(12):212–7. Chinese.
[7] Wang W, Zhao Y, Jiang C, Yue H, Li X. Ride comfort of vehicle on new mechanical elastic wheel. China Mech Eng 2013;24(22):3114–7, 3123. Chinese.
[8] Pan X, Wang D, Lin Y, Chen X. An analysis on the compliance steering characteristics of five-link dependent rear suspension with multi-body dynamics. Automot Eng 2013;35(4):332–5. Chinese.
[9] Li X, Chen W, Chen X. Research on vehicle suspension NVH performance based on flexiabie–rigid coupling model. China Mech Eng 2014;25(7):978–83. Chinese.
[10] Zhao T, Li C, Wang J. Fatigue life analysis of a mini truck body based on FEM. Automot Eng 2011;33(5):428–32. Chinese.
[11] Cook RD, Malkus DS, Plesha ME. Concepts and applications of finite element analysis. Hoboken: John Wiley & Sons; 1989.
[12] Zang M, Duan F, Zhou T, Yu S. FEM simulation analysis and estimation on wet-road braking distance of complex-patterned tire. China Mech Eng 2013;24(16):2257–61. Chinese.
[13] Zang M, Zhang B. FEM simulation and evaluation on tire braking performance. Automot Eng 2014;36(6):699–708. Chinese.
[14] Chen K, Gao J, Lv Z. VPG based simulation and analysis on vehicle driving comfort. Chinese J Constr Mach 2010;8(2):208–12. Chinese.
[15] Chen K, Gao J, He H. VPG based simulation and analysis on vehicle side crash. Chinese J Constr Mach 2010;8(4):449–54. Chinese.
[16] Hu Y, Zhou H, Xu G. Study on virtual test rig for vehicle road simulation test. Chinese J Automot Eng 2014;4(2):137–42.
[17] Duni E, Toniato G, Saponaro R, Smeriglio P, Puleo V. Vehicle dynamic solution based on finite element tire/road interaction implemented through implicit/explicit sequential and co-simulation approach. SAE Tech Pap 2010:2010-01-1138.
[18] Hibbitt, Karlsson, and Sorensen, Inc. ABAQUS example problems manual. Pawtucket: Hibbitt, Karlsson & Sorensen, Inc; 2002.
[19] Hibbitt, Karlsson, and Sorensen, Inc. ABAQUS theory manual. Pawtucket: Hibbitt, Karlsson & Sorensen, Inc; 2003.
[20] ABAQUS, Inc. ABAQUS analysis user's manual. Providence: ABAQUS, Inc.; 2015.
[21] Overview of the test field [Internet]. Chongqing: Chongqing Xibu Automobile Proving Ground Management Co., Ltd.; c2004–2012 [cited 2018 May 20]. Available from: http://www.cxapg.com/.